ISBN: 978-3-95450-232-5 ISSN: 2673-7000 doi:10.18429/JACoW-NAPAC2022-MOZD2

PRELIMINARY STUDY OF A HIGH GAIN THz FEL IN A RECIRCULATING CAVITY*

A. Fisher†, P. Musumeci
Department of Physics and Astronomy, University of California Los Angeles, CA, USA

Abstract

Recent experimental results have shown a large improvement in the single pass efficiency of an FEL at 160 GHz by introducing a waveguide to match the average electron longitudinal velocity to the subluminal radiation group velocity. We now consider the possibility of using a cavity to recirculate a portion of the THz radiation to seed successive electron bunch passes through the undulator. The effects of waveguide dispersion are discussed along with a method to correct the group velocity delay of the radiation pulse. Finally, we simulate power outcoupling for four electron beam passes and evaluate the benefit of dispersion correction.

INTRODUCTION

Among the electromagnetic radiation sources in the 0.1-10 THz frequency range, FELs have the unique ability to provide high peak and average power at tunable frequencies with repetition rates limited only by the availability of electron beams. While FEL lasing conditions are relaxed at longer wavelengths, radiation diffraction and FEL slippage reduce the interaction length and gain for a single pass. For this reason, most operating and planned THz FEL facilities employ cavity designs where the gain can be increased over hundreds of micropulses [1–6].

A promising option to increase the single pass gain is a THz waveguide FEL where the radiation group velocity is tuned to match the average longitudinal velocity of the electron beam, eliminating slippage effects. The electron beam can then be compressed without limit, increasing the peak current and making it possible to seed the interaction with a large bunching factor. Recent experimental results have demonstrated 10% average energy extraction from a 5.5 MeV electron beam in a 1-meter undulator [7]. In this high gain regime, the interaction quickly saturates and significant tapering of the undulator parameters is necessary to maintain the resonant conditions [8].

The efficiency can be increased further by recirculating a fraction of the produced THz radiation to seed the interaction of successive electron bunches [9, 10]. This could increase the frequency range of the waveguide FEL as the gain is limited at higher frequencies by wakefield effects, smaller bunching factors, and reduced charge transmission. Additionally, it could compensate for cases where the electron beam brightness is insufficient to achieve large energy extraction in a single pass.

The article is organized as follows. First we discuss a preliminary cavity design for the Pegasus beamline including comments on undulator tapering. Next we present ideal simulations with no outcoupling to emphasize the benefit of seeding with radiation. Finally, we discuss a method for dispersion correction and its effect on the interaction at different power outcoupling fractions.

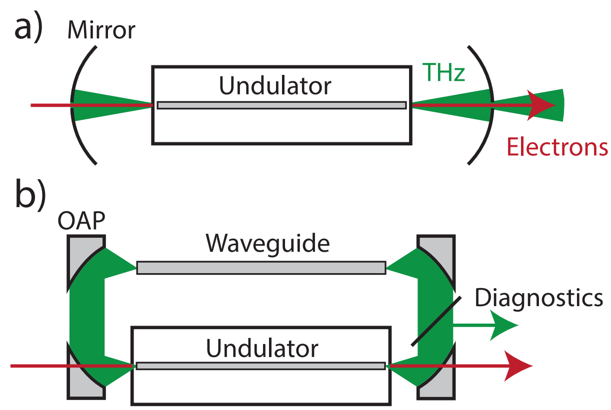

Figure 1: Two cavity designs for the Pegasus beamline with differing complexity.

CAVITY DESIGN

Figure 1 shows two possible cavity designs for the Pegasus beamline at UCLA where space constraints in the bunker restrict the electron beam path to a straight line. Electron bunches are generated by illuminating a Cu photocathode in a RF gun with a 40 fs laser pulse. Multiple beams with tunable delay (necessary to inject electron bunches at the decelerating radiation phase) can be produced by separating the pulse with polarizing beamsplitters and using tunable delay lines.

The first cavity design consists of two concave mirrors on either side of the undulator. A small hole in the upstream mirror is needed to accommodate the focused, incoming electron beam and the radiation is outcoupled with a larger hole in the downstream mirror. The simple design is appealing, but the radiation will experience significant waveguide dispersion on the return trip reducing the peak electric field that can seed the next pass. A more complicated but versatile design uses an off-axis parabolic (OAP) mirror to reflect the THz radiation outside the beamline. An outcoupling THz beamsplitter reflects some radiation to a diagnostics section for spectral and temporal measurements. A second waveguide (with larger radius to reduce dispersion) confines the radiation and limits diffraction losses of the large bandwidth pulse. We can easily switch between multiple pass measurements and single pass measurements by replacing

* This work was supported by DOE grant No. DE-SC0009914.
† afisher000@g.ucla.edu

ISBN: 978-3-95450-232-5 ISSN: 2673-7000 doi:10.18429/JACoW-NAPAC2022-MOZD2

the outcoupling beamsplitter with a mirror. However, the complexity introduces more opportunities for THz losses due to misalignment, lossy vacuum windows, and inefficient matching between waveguide and free-space radiation modes.

Undulator tapering is an important aspect of the cavity design. In a single pass FEL, the undulator field is simply tapered to maintain resonance with the decelerated electrons. For multiple high gain passes, a trade off exists between the gain achieved in the first pass and the maximum efficiency when the gain saturates.

It is instructive to consider a 1D (single frequency) model for a high efficiency FEL interaction [11]. Assuming no seed radiation and approximately constant bunching, the radiation field grows linearly in z, requiring a quadratic tapering of the undulator field. At the other extreme, for strong seeding we can assume the radiation field remains approximately constant as the field growth is effectively offset by waveguide dispersion. In this constant field limit, the ideal tapering is linear. The best tapering for many passes would tend to the linear tapering limit as the gain builds over time. For our experiment considering several passes, the ideal tapering will include a mix of linear and quadratic terms.

Table 1: Experiment Parameters

Electron Beam		Undulator/Waveguide	
Q	125 pC	$K_{rms,0}$	2.18
γ	14.5	λ_u	3.2 cm
σ_γ/γ	0.7%	N_u	30
σ_x, σ_y	139 µm, 122 µm	WG material	Cu
σ_z	90 μm	WG Radius	1.6 mm
$\epsilon_{n,x}, \epsilon_{n,y}$	5 mm·mrad		

RECIRCULATION

Simulations were carried out with the GPTFEL extension for the General Particle Tracer code (GPT) which expands the radiation field into a basis of frequency and spatial waveguide modes [12]. The simulation parameters in Table 1 are borrowed from a follow-up high efficiency single pass experiment targeting 330 GHz where a solenoid and permanent magnet chicane have been added to the beamline to improve beam compression and matching into the undulator [13].

At full charge transmission with 125 pC, a single pass can achieve greater than 20% efficiency. To better highlight the effects of recirculation, we study the case in which the laser is used to generate 80 pC bunches at the cathode.

The undulator field tapering given by

$$B(z) = B_0 \quad \text{for} \quad z < z_0$$
$$B(z) = B_0(1 - 0.2z(m) - 0.35z(m)^2) \quad \text{for} \quad z \geq z_0 \quad (1)$$

where B_0 = 730 mT, was selected using a numerical scan of the tapering parameters for simulations of three undulator passes. Tapering parameters included the linear and quadratic terms along with the taperdelay, z_0 = 5 cm.

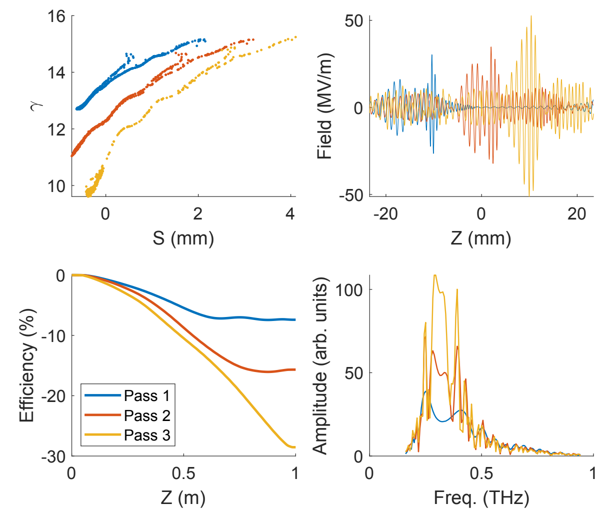

Figure 2: Simulation results for three electron bunch passes with no outcoupling. Temporal profiles are offset to ease visibility.

Figure 2 shows the electron beam and radiation properties for three undulator passes with no outcoupling. The efficiency increases significantly with each pass as the growing seed field causes the electrons to stay in resonance with the undulator tapering for longer distances. As electrons drop out of resonance they begin to slip in phase and can absorb energy from the radiation, creating the dip in the spectrum and double peaks in the temporal profile. This ideal simulation neglects cavity losses, but highlights the large energy extraction that can be unlocked by seeding with THz radiation.

DISPERSION CORRECTION

The efficiency for a given pass is directly correlated to the peak electric field of the seed radiation as the electron beam is compressed to less than a radiation wavelength. By compensating for waveguide dispersion, we could achieve larger peak fields and therefore larger efficiencies, especially in the presence of cavity losses.

One option involves constructing a layered dielectric structure on top of a totally reflective surface, forming a multilayer Gires-Tournois interferometer or MGTI [14]. The layer material and thicknesses can be chosen to provide phase delays that offset the THz dispersion. Larger compensation over a broader range of frequencies can be achieved by using multiple MGTIs in series.

The group velocity delay of a signal is defined as the derivative of the phase with respect to angular frequency. We can solve for the induced phase of a reflected wave off an MGTI by enforcing boundary conditions on the fields at each surface. The induced phase $E_{ref} = E_{inc}e^{i\phi}$ is given

ISBN: 978-3-95450-232-5 ISSN: 2673-7000 doi:10.18429/JACoW-NAPAC2022-MOZD2

by

$$\phi = -i \ln \left(\frac{R_{21} - R_{22}}{R_{11} - R_{12}} \right) \quad \text{where} \quad R = \prod_{j=1}^{N} R_j$$

$$\text{and} \quad R_j = \frac{1}{2} \begin{pmatrix} \exp(-i\psi_j)\xi_j^+ & \exp(i\psi_j)\xi_j^- \\ \exp(-i\psi_j)\xi_j^- & \exp(i\psi_j)\xi_j^+ \end{pmatrix} \quad (2)$$

where $\xi^\pm = 1 \pm \frac{n_j}{n_{j-1}}$, $\psi_j = n_j d_j \omega / c$, and n_j, d_j are the index of refraction and thickness of the j^{th} layer. These expressions can be extended to non-normal incidence by replacing $d_j \rightarrow d_j / \cos(\theta_j)$ where θ_j is the radiation angle, and using $\xi_S^\pm = 1 \pm \frac{n_j \cos(\theta_j)}{n_{j-1}\cos(\theta_{j-1})}$ or $\xi_P^\pm = \frac{\cos(\theta_j)}{\cos(\theta_{j-1})} \pm \frac{n_j}{n_{j-1}}$ for S and P polarizations, respectively.

To design our MGTI structures, we need to compute the group velocity delay for our simulated THz pulses. GPTFEL outputs the amplitude, phase, frequency, and longitudinal phase number (denoted A, ϕ, f and k_z, respectively) at each timestep. The waveform At_{00} at a given timestep is evaluated along the vector z_{00} which is defined by the frequency range and number of spatial frequency modes used by the simulation. For example, the temporal pulse at final time t_f is given by

$$At_{00} = \sum_m A_{m,f} dN \cos(\phi_{m,tot}) \quad \text{with} \quad (3)$$

$$\phi_{m,tot} = k_{z,m}(z_{00} + ct_f + dz) - \omega_m t_f + \phi_{m,f} \quad (4)$$

where m labels the frequency modes, dN is the number of real frequency modes represented by each simulation mode, $\omega = 2\pi f$, and dz represents the pulse position relative to the waveguide center at $t = 0$. The term $k_z ct_f$ is responsible for moving the reference frame at the speed of light.

The waveform can be used to seed another electron bunch in a simulation starting at $t = t_i$ by defining $A_{m,i} = A_{m,f}$ and $\phi_{m,i} = \phi_{m,tot} - k_{z,m}(ct_i + dz) + \omega_m t_i$. Additionally, the waveform can be shifted a distance Δz in $\hat{z}$ by adding the phase $-k_{z,m} z_0$ to $\phi_{m,tot}$.

To compute the group velocity delay for our waveform, one must "unwind" the total phases $\phi_{m,tot}$ from being defined in $[-\pi, \pi)$ and numerically differentiate with respect to angular frequency. Figure 3 shows the inverse of the calculated group velocity delay for the first pass through the undulator along with the correction from two MGTI structures made with alternating layers of silicon and air. After compensating the group velocity delay, the corrected $\phi_{m,tot}$ is found by numerically integrating with respect to angular frequency.

Figure 4 shows the results of the dispersion correction from Fig. 3. Because the MGTI structure was only designed to compensate frequencies within ≈ 100 GHz of the resonant frequency, the pulse still has long dispersed tails. However, the two temporal peaks in the original signal have now merged. It should be noted that while the field is larger at the two peaks than at $Z = 0$, the peak frequencies are higher and lower than the resonant frequency and will not

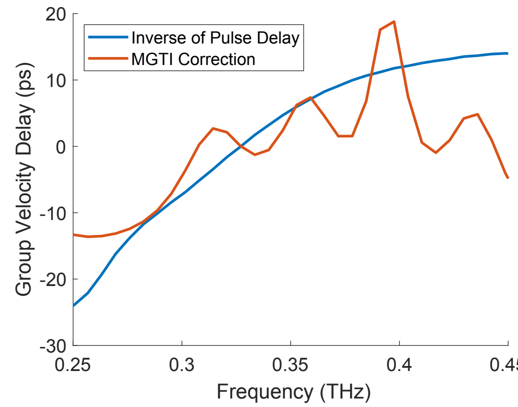

Figure 3: Fitting the inverse of the THz dispersion with two MGTI structures. First structure has two layers: 130 µm Si, 780 µm air. Second structure has four layers: 110 µm Si, 760 µm air, 50 µm Si, 140 µm air.

efficiently couple with an electron beam in successive passes. Thus, comparing the field strengths at $Z = 0$, we see that the MGTI correction has increased the THz field by at least a factor of 2.

As long as efficient energy exchange occurs between the electrons and the radiation in the undulator, the effect of waveguide dispersion is limited, similar to gain guiding in free space FELs. Only when electrons fall out of resonance do we see strong dispersive signatures. For this reason, we expect the benefits of dispersion correction to diminish as the efficiency increases.

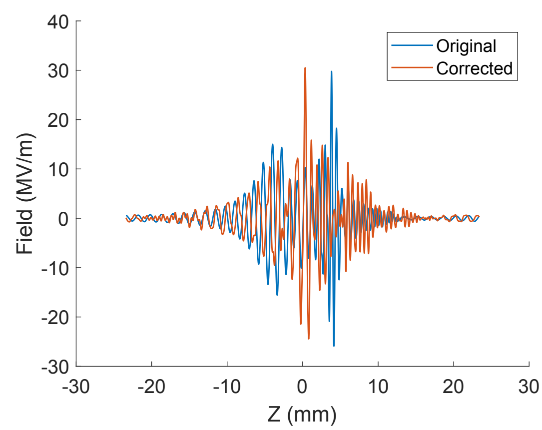

Figure 4: MGTI correction of THz waveform from first undulator pass.

OUTCOUPLING

A THz cavity must outcouple a certain fraction of power in each pass. Figure 5 shows the efficiencies for undulator passes with and without MGTI disperison correction for a range of power outcouplings (first pass is same for all and therefore not shown). The outcoupling was applied by

ISBN: 978-3-95450-232-5 ISSN: 2673-7000 doi:10.18429/JACoW-NAPAC2022-MOZD2

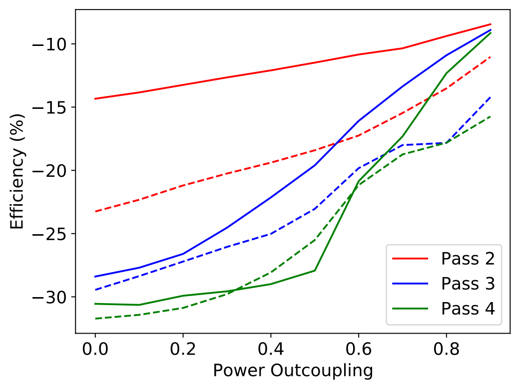

Figure 5: Efficiency of undulator passes with (dotted line) and without (solid line) dispersion correction for different power outcoupling fractions.

scaling the mode amplitudes by a factor of $\sqrt{1 - P_{out}}$ where P_{out} is the fraction of power removed from the cavity.

The benefit of dispersion correction is greatest for passes with low gain where the waveguide dispersion effect is largest. At low power outcoupling, there is negligible benefit as the interaction begins to saturate after only a few passes (efficiency limited by undulator tapering). However at outcoupling fractions greater than 0.6, dispersion correction allows each pass to maintain efficiencies of $\sim$ 17% while the efficiencies of the uncorrected passes converge to the zero-seed limit ($\sim$ 8%).

Assuming a saturated efficiency of 30% for an outcoupling fraction of 0.5, the amount of energy outcoupled per pass is twice that produced by a single pass design.

CONCLUSION

The single pass gain of a high efficiency waveguide FEL can be limited by available electron beam brightness along with wakefield effects and reduced charge transmission at higher frequencies. In these cases, a cavity that recirculates a portion of the radiation to seed successive electron bunches significantly increases the possible energy extraction from each pulse. Pulse dispersion from the waveguide (strongest for lower gain passes) can be compensated using MGTI structures to increase the peak field, achieving gain saturation in fewer passes and improving efficiency for large power outcoupling. Simulations using nominal experiment parameters at a reduced charge suggest the outcoupled THz energy per pulse of a recirculating cavity is twice that of a single pass design.

REFERENCES

[1] D. Oepts, A. Van der Meer, and P. Van Amersfoort, "The free-electron-laser user facility FELIX," *Infrared Physics & Technology*, vol. 36, no. 1, pp. 297–308, 1995. doi:10.1016/1350-4495(94)00074-U

[2] Y. U. Jeong *et al.*, "First lasing of the kaeri compact far-infrared free-electron laser driven by a magnetron-based microtron," *Nucl. Instrum. Methods Phys. Res., Sect. A*, vol. 475, no. 1-3, pp. 47–50, 2001. doi:10.1016/S0168-9002(01) 01533-9

[3] B. A. Knyazev, G. N. Kulipanov, and N. A. Vinokurov, "Novosibirsk terahertz free electron laser: Instrumentation development and experimental achievements," *Measurement Science and Technology*, vol. 21, no. 5, p. 054 017, 2010. doi:10.1088/0957-0233/21/5/054017

[4] X. Shu, Y. Dou, X. Yang, M. Li, H. Wang, and X. Lu, "First lasing of CAEP THz FEL facility," in *2017 42nd International Conference on Infrared, Millimeter, and Terahertz Waves (IRMMW-THz)*, IEEE, 2017, pp. 1–2. doi:10.1109/IRMMW-THz.2017.8067077

[5] H.-T. Li, Q.-K. Jia, S.-C. Zhang, L. Wang, and Y.-L. Yang, "Design of FELiChEM, the first infrared free-electron laser user facility in china," *Chinese Physics C*, vol. 41, no. 1, p. 018 102, 2017. doi:10.1088/1674-1137/41/1/018102

[6] A. Nause *et al.*, "6 MeV novel hybrid (standing wave-traveling wave) photo-cathode electron gun for a THz superradiant FEL," *Nucl. Instrum. Methods Phys. Res., Sect. A*, p. 165 547, 2021. doi:10.1016/j.nima.2021.165547

[7] A. Fisher *et al.*, "Single-pass high-efficiency terahertz free-electron laser," *Nature Photonics*, pp. 1–7, May 2022. doi:10.1038/s41566-022-00995-z

[8] J. Duris, A. Murokh, and P. Musumeci, "Tapering enhanced stimulated superradiant amplification," *New Journal of Physics*, vol. 17, no. 6, p. 063 036, 2015. doi:10.1088/ 1367-2630/17/6/063036

[9] J. Duris, P. Musumeci, N. Sudar, A. Murokh, and A. Gover, "Tapering enhanced stimulated superradiant oscillator," *Phys. Rev. Accel. Beams*, vol. 21, p. 080 705, 8 Aug. 2018. doi:10.1103/PhysRevAccelBeams.21.080705

[10] R. L. Sheffield, D. C. Nguyen, J. C. Goldstein, N. A. Ebrahim, C. M. Fortgang, and J. M. Kinross-Wright, "Compact 1-kW infrared regenerative amplifier FEL," in *Free-Electron Laser Challenges*, P. G. O'Shea and H. E. Bennett, Eds., International Society for Optics and Photonics, vol. 2988, SPIE, 1997, pp. 28–37. doi:10.1117/12.274394

[11] C. Emma, N. Sudar, P. Musumeci, A. Urbanowicz, and C. Pellegrini, "High efficiency tapered free-electron lasers with a prebunched electron beam," *Physical Review Accelerators and Beams*, vol. 20, no. 11, p. 110 701, 2017. doi:10.1103/ PhysRevAccelBeams.20.110701

[12] A. Fisher, P. Musumeci, and S. Van der Geer, "Self-consistent numerical approach to track particles in free electron laser interaction with electromagnetic field modes," *Physical Review Accelerators and Beams*, vol. 23, no. 11, p. 110 702, 2020. doi:10.1103/PhysRevAccelBeams.23.110702

[13] A. C. Fisher *et al.*, "Simulating Beam Transport with Permanent Magnet Chicane for THz Fel," 13, presented at IPAC'22, Bangkok, Thailand, Jun. 2022, paper TUPOPT032, unpublished.

[14] K. Strecker, S. Ekin, and J. F. O'Hara, "Compensating atmospheric channel dispersion for terahertz wireless communication," *Scientific reports*, vol. 10, no. 1, pp. 1–8, 2020. doi:10.1038/s41598-020-62692-7